

pubs.acs.org/NanoLett Letter

Vibrational Anharmonicity and Energy Relaxation in Nanoscale Acoustic Resonators

Cameron Wright and Gregory V. Hartland*



Cite This: Nano Lett. 2023, 23, 11161-11166



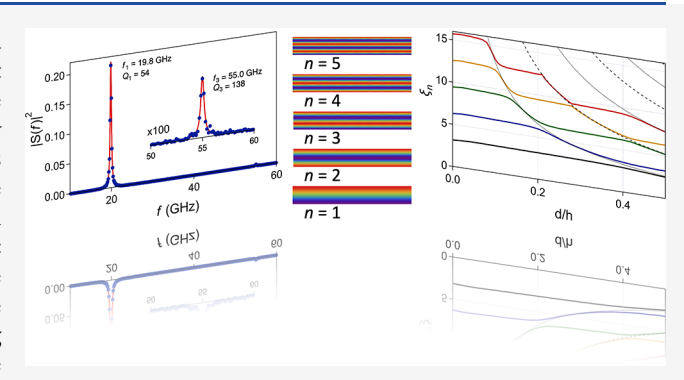
ACCESS I

III Metrics & More

Article Recommendations

Supporting Information

ABSTRACT: The fundamental and n=3 overtones of Au nanoplate thickness vibrations have been studied by transient absorption microscopy. The frequencies of the n=3 overtone are less than $3\times$ the frequency of the fundamental. This anharmonicity is explained through a continuum mechanics model that includes organic layers on top of the nanoplate and between the nanoplate and the glass substrate. In this model, anharmonicity arises from coupling between the vibrations of the nanoplate and the organic layers, which creates avoided crossings that reduce the overtone frequencies compared to the fundamental. Comparison of the experimental and calculated quality factors shows that coupling occurs to the top organic layer. Good agreement between the measured and calculated quality factors is obtained by introducing



internal damping for the nanoplate. These results show that engineering layers of soft material around metal nanostructures can be used to control the vibrational lifetimes.

KEYWORDS: transient absorption microscopy, plasmonics, acoustic modes, nanomaterials

Tanoscale materials display vibrational modes with frequencies ranging from the MHz to THz depending on the dimensions and composition of the material and the identity of the mode. These modes have been used in applications such as detection of the optical absorption of single molecules,² measurements of the mass of single nanoobjects,^{3,4} force sensing,⁵ and as probes of the frequency dependent mechanical properties of materials.⁶ In these applications it is important to understand and control the damping of the vibrational modes.⁷⁻⁹ The majority of the applications use suspended nanostructures in order to reduce environmental damping from the radiation of sound waves into the substrate. High vibrational quality factors have also been achieved by using low density substrates, 10 manipulating the aspect ratio of the nanostructure, 11 or by introducing a spacer layer between the nanostructure and the substrate. 12 The use of a spacer layer to increase the vibrational lifetimes is an appealing approach from a device fabrication point-of-view; however, the maximum quality factors that can be created in this way are not well understood.

Recently we used transient absorption microscopy (TAM) to measure the vibrational response of a gold nanoplate drop cast onto a glass substrate. Long lived vibrational modes were observed, even though there was no special preparation of the substrate. The nanoplate also displayed up to n = 7 overtone modes, see also ref 14, with frequencies that were almost exact integer multiples of the fundamental breathing mode frequency. The lifetimes of the overtone modes were

significantly smaller than that of the fundamental. These observations were explained using a continuum mechanics model, where there is a low-density spacer layer between the nanoplate and the substrate. This analysis showed that the nanoplate in ref 13 behaved more like a free plate than a plate attached to a solid substrate. The high quality factors and multiple overtones for this nanoplate are atypical; usually metal nanostructures on solid substrates have quality factors less than 20, 1,15-19 and multiple overtone modes are typically not observed.

In this paper, we investigate the damping of the fundamental compared to the n=3 overtone mode for a series of nanoplates. The data shows several differences to the special nanoplate discussed in ref 13. First, the nanoplates in general display anharmonicity: the overtone frequencies are smaller than integer multiples of the fundamental, in contrast to the results in ref 13. The overtone modes also have quality factors higher than those of the fundamental mode. These results can be accounted for by a continuum mechanics model that consists of an organic "spacer" layer between the substrate and

Revised: September 22, 2023 Revised: November 16, 2023 Accepted: November 16, 2023

Published: November 20, 2023





Nano Letters pubs.acs.org/NanoLett Letter

the nanoplate, and a second organic layer on top of the nanoplate. This work provides important insights into controlling nanoplate vibrational quality factors, which is potentially useful for the development of nanoelectromechanical devices for sensing applications.

The samples in the experiments were prepared by drop casting a nanoplate solution onto a glass coverslip. Individual nanoplates were identified under a microscope and interrogated by transient absorption microscopy using a Menlo Systems Dual Color 520/780 Asynchronous Optical Sampling (ASOPS) system; ^{21,22} see the Supporting Information for details. The nanoplates were excited at 780 nm and probed at 520 nm. Ultrafast heating from the pump laser excites the breathing modes of the structures, which produce modulations in the transient absorption traces. ^{1,15} Vibrational spectra were obtained by Fourier transforming the transient absorption traces using the Fast Fourier Transform (FFT) routine implemented in IgorPro (version 9.02), using the magnitude squared output.

Before presenting the experimental data, it is helpful to review the continuum mechanics results for the breathing modes of an isolated nanoplate (no substrate) and a nanoplate on a substrate with no spacer layer. 16,20,23,24 For isolated nanoplates, the frequencies depend on the boundary conditions which can be free (zero stress) or fixed (zero displacement). For a nanoplate with homogeneous boundary conditions, i.e., both surfaces free or both fixed, the breathing mode frequencies are $\omega_n = n\pi c_1/h$, where c_1 is the speed of sound in the nanoplate, h is the thickness and n = 1, 2, 3, ...When one surface is fixed and the other is free the frequencies are $\omega_n = \left(n - \frac{1}{2}\right)\pi c_1/h$. For a nanoplate on a lower acoustic impedance substrate (for example, gold on glass), the frequencies are the same as those for an isolated nanoplate with homogeneous boundary conditions. Conversely, when the acoustic impedance of the substrate is larger than that of the nanoplate, the frequencies are the same as those for an isolated nanoplate with mixed boundary conditions (see the Supporting Information for more details). For a supported nanoplate the quality factors of the vibrational modes depend sensitively on the difference in acoustic impendence $(Z = \rho c_1)$ between the nanoplate and the substrate, with larger quality factors obtained for large ΔZ . It is also important to note that in general only the odd order modes are observed in transient absorption experiments on nanoplates, 13,14 as these are the ones that correspond to volume changes.²³

Figure 1 shows vibrational spectra of two nanoplates on a glass coverslip obtained by Fourier transformation of the transient absorption microscopy traces. In Figure 1a excitation is through the glass, and in Figure 1b excitation is through the air. The peaks labeled n = 1 and n = 3 are assigned to the fundamental and third overtone of the nanoplate breathing mode. The peak labeled with an asterisk ("*") in Figure 1a corresponds to Brillouin oscillations in the glass. 25,26 This peak does not appear when the sample is excited through air. The red lines in Figure 1 show Lorentzian fits to the data. The frequencies f_i and quality factors $Q_n = f_n/\Delta f_n$ from the fitting procedure are $f_1 = 20.10 \pm 0.01$ GHz, $Q_1 = 11.6 \pm 0.1$, $f_3 =$ 59.25 ± 0.02 GHz, and $Q_3 = 52 \pm 4$ for the data in Figure 1a and f_1 = 19.85 \pm 0.01 GHz, Q_1 = 53.8 \pm 0.1, f_3 = 54.99 \pm 0.02 GHz, and $Q_3 = 138 \pm 18$ for the data in Figure 1b. Note that the errors from the fitting routine can be unreasonably small (much less than the spacing between points for the

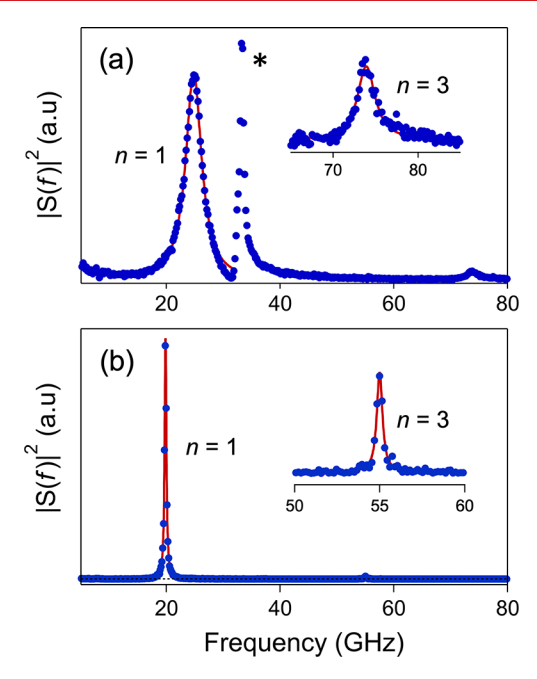


Figure 1. Vibrational spectra of two different nanoplates determined from Fourier transforming single nanoparticle transient absorption microscopy data. (a) Sample excited through the glass coverslip and (b) sample excited through air. The peak labeled "*" in panel (a) is assigned to Brillouin oscillations in the glass. The red lines are Lorentzian fits to the data.

frequencies, for example). Thus, for the analysis presented below, errors were determined from multiple measurements of the frequencies and quality factors for a representative nanoplate; see the Supporting Information for details.

The two nanoplates in Figure 1 show very differ behavior. The strongly damped nanoplate in Figure 1a is relatively harmonic $(f_3 = 2.98f_1)$, whereas, the high quality factor nanoplate in Figure 1b displays significant anharmonicity (f_3 = $2.77f_1$). To further investigate the relationship between anharmonicity and damping, a number of nanoplates were interrogated. We obtained good data for 14 nanoplates where both the fundamental and the n = 3 overtone could be clearly observed in the vibrational spectrum. Several nanoplates also showed the n = 5 mode, however, not enough to create a reliable data set. Thus, in the following we concentrate on the relationship between the frequencies and quality factors of the fundamental and n = 3 overtone. Figure 2a shows the n = 3overtone frequency (f_3) plotted versus the fundamental frequency (f_1) . The large spread in f_1 values is attributed to the different thickness nanoplates present in the sample. The important point from this figure is that the overtone frequency is always less than or equal to 3× the fundamental frequency $(f_3 \le 3f_1)$. We believe that this anharmonicity arises from the presence of organic material either between the nanoplate and the substrate or on-top of the nanoplate. The nanoplate modes hybridize with the vibrational mode of these organic layers, 20,23 which causes a decrease in the overtone frequencies.

Figure 2b shows the quality factors versus normalized frequency $(Q_n \text{ versus } f_n/n)$ for the fundamental and n=3 overtone. The dashed horizontal lines are the expected quality factors for a nanoplate on a glass surface without a spacer layer. The data show large variance in the quality factors from the different nanoplates. The values of Q_3 are in general higher than those for Q_1 . This is in contrast to our previous paper, ¹³

Nano Letters pubs.acs.org/NanoLett Letter

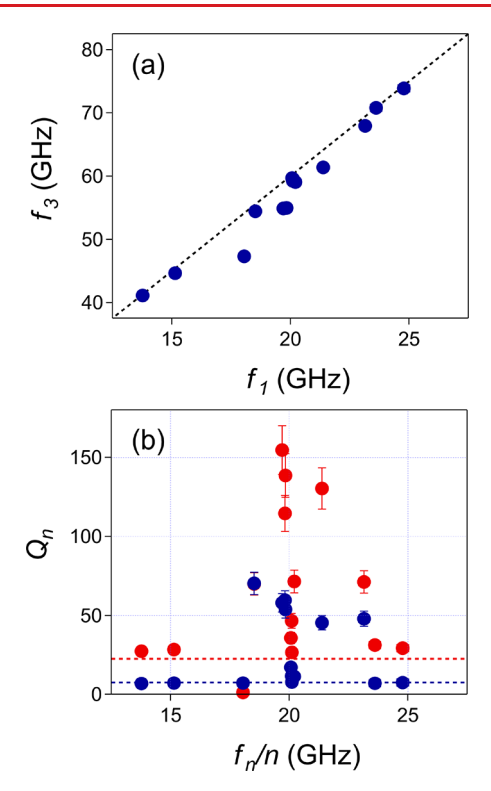


Figure 2. (a) Plot of the frequency of the n = 3 overtone (f_3) versus the frequency of the fundamental breathing mode (f_1) . (b) Quality factor Q_n versus f_n/n for the fundamental and n = 3 overtone. Blue = fundamental; red = overtone. The horizontal dashed lines in panel (b) are the Q_n values for a nanoplate on a glass surface without organic layers.

where the fundamental was observed to have a much longer lifetime than that of the overtone modes (in this respect the nanoplate examined in ref 13 is an anomaly).

To understand these results, the continuum mechanics model for a nanoplate on a surface was extended to include an organic spacer layer between the nanoplate and the substrate, with and without a second organic layer on top. See Figure 3 below for a diagram of the two models. Note that results for the spacer layer without the top layer have been previously discussed in refs 12 and 20. For a single spacer layer the vibrational frequencies and quality factors are obtained by solving the eigenvalue equation

$$\tan\left[\xi_{n}\right] \frac{c_{1}\rho_{1}}{c_{2}\rho_{2}} \left(i + \tan\left[\frac{c_{1}d}{c_{2}h}\xi_{n}\right] \frac{c_{3}\rho_{3}}{c_{2}\rho_{2}}\right) + i \tan\left[\frac{c_{1}d}{c_{2}h}\xi_{n}\right] - \frac{c_{3}\rho_{3}}{c_{2}\rho_{2}} = 0$$
(1)

where $\xi_n = \omega h/c_1$ is the scaled frequency, d and h are the thicknesses of the organic layer and nanoplate, respectively, and c_i and ρ_i are the longitudinal speed of sound and the density of the material (i = 1 for the Au, i = 2 for the organic material, and i = 3 for the glass). The frequencies and quality factors are obtained from $f_n = c_1 \text{Re}[\xi_n]/(2\pi h)$ and $Q_n = \text{Re}[\xi_n]/(2\text{Im}[\xi_n])$. For a nanoplate with a spacer layer and a top layer the above eigenvalue equation is modified to

$$\begin{aligned} &\tan[\xi_n] \sin\left[\frac{c_1d}{c_2h}\xi_n\right] \left(\sin\left[\frac{c_1d}{c_2h}\xi_n\right] \frac{c_2\rho_2}{c_1\rho_1} + i\cos\left[\frac{c_1d}{c_2h}\xi_n\right] \frac{c_3\rho_3}{c_2\rho_1}\right) \\ &- \sin\left[2\frac{c_1d}{c_2h}\xi_n\right] - i\cos\left[2\frac{c_1d}{c_2h}\xi_n\right] \frac{c_3\rho_3}{c_2\rho_2} \\ &+ \cos\left[\frac{c_1d}{c_2h}\xi_n\right] \tan[\xi_n] \frac{c_1\rho_2}{c_2\rho_2} \left(-\cos\left[\frac{c_1d}{c_2h}\xi_n\right] + i\sin\left[\frac{c_1d}{c_2h}\xi_n\right] \frac{c_3\rho_3}{c_2\rho_2}\right) = 0 \end{aligned}$$

The derivations of eqs 1 and 2 are presented in the Supporting Information. Note that we have assumed for simplicity that the spacer layer and the top organic layer have the same thickness.

Figure 3 shows the eigenvalues and quality factors calculated

from eqs 1 and 2 for the gold nanoplate/organic layer/glass substrate system as a function of d/h. The eigenvalues show a series of avoided crossings that occur when the nanoplate modes $(\xi_n = n\pi)$ come into resonance with the modes of the organic layers.^{20,23} For the case of a single spacer layer (Figure 3a) the organic layer modes that appear are at the frequencies for a layer with homogeneous boundary conditions: $\omega_n = n\pi c_2/$ d corresponding to $Re[\xi_n] = n\pi c_2 h/(c_1 d)$ on the eigenvalue plot in Figure 3 (shown as the dashed lines in Figure 3a). Adding a top organic layer (Figure 3b) introduces a second set of organic layer modes with frequencies commensurate with the vibrations of a layer under mixed boundary conditions. These frequencies follow $\omega_n = \left(n - \frac{1}{2}\right)\pi c_2/d$ and appear at $\operatorname{Re}[\xi_n] = \left(n - \frac{1}{2}\right)\pi c_2 h/(c_1 d)$ (plotted as the dotted lines in Figure 3b). At the avoided crossings, the vibrational frequencies of the overtone modes of the nanoplate decrease relative to the fundamental, which provides an explanation for the anharmonicity observed in Figure 2a. Note that an analogous effect has previously been observed for spherical Au nanoparticles coupling to the modes of a SiO₂ shell.^{27,28} For the Au nanoparticle-SiO₂ shell system, it was possible to

The quality factors for the two models are presented in Figure 3c,d. The calculations show that the quality factors initially increase with increasing thickness of the organic layer for both models. However, there are significant differences in the Q_n values in the avoided crossing regions for the spacer layer only model compared with the two layer model. When the vibrational modes of the nanoplate mix with modes of the spacer layer (Figure 3c and the second set of avoided crossings in Figure 3d), they are strongly damped. In contrast, when the nanoplate modes mix with the modes of the top layer (first set of avoided crossings in Figure 3d), the quality factors increase. For the experimental data, the quality factors of the n = 3overtone are in general larger than those of the fundamental. This means that the two-layer model is the correct description of the data, and that the nanoplate vibrations hybridize with the modes of the top organic layer.

observe both increases and decreases in vibrational frequencies

from the avoided crossings, whereas only decreases are

observed for the nanoplates in our experiments.

To quantitatively compare the experimental quality factors to the simulations, the quality factors are plotted versus (f_3/f_1) – 3 in Figure 4. This quantity is a measure of the degree of anharmonicity $((f_3/f_1) - 3 = 0$ for harmonic vibrations and $(f_3/f_1) - 3 < 0$ for anharmonic vibrations). The solid lines in Figure 4 show the continuum mechanics results for the fundamental (blue) and n = 3 overtone (red). The dotted horizontal lines are the quality factors for a nanoplate on a

Nano Letters pubs.acs.org/NanoLett Letter

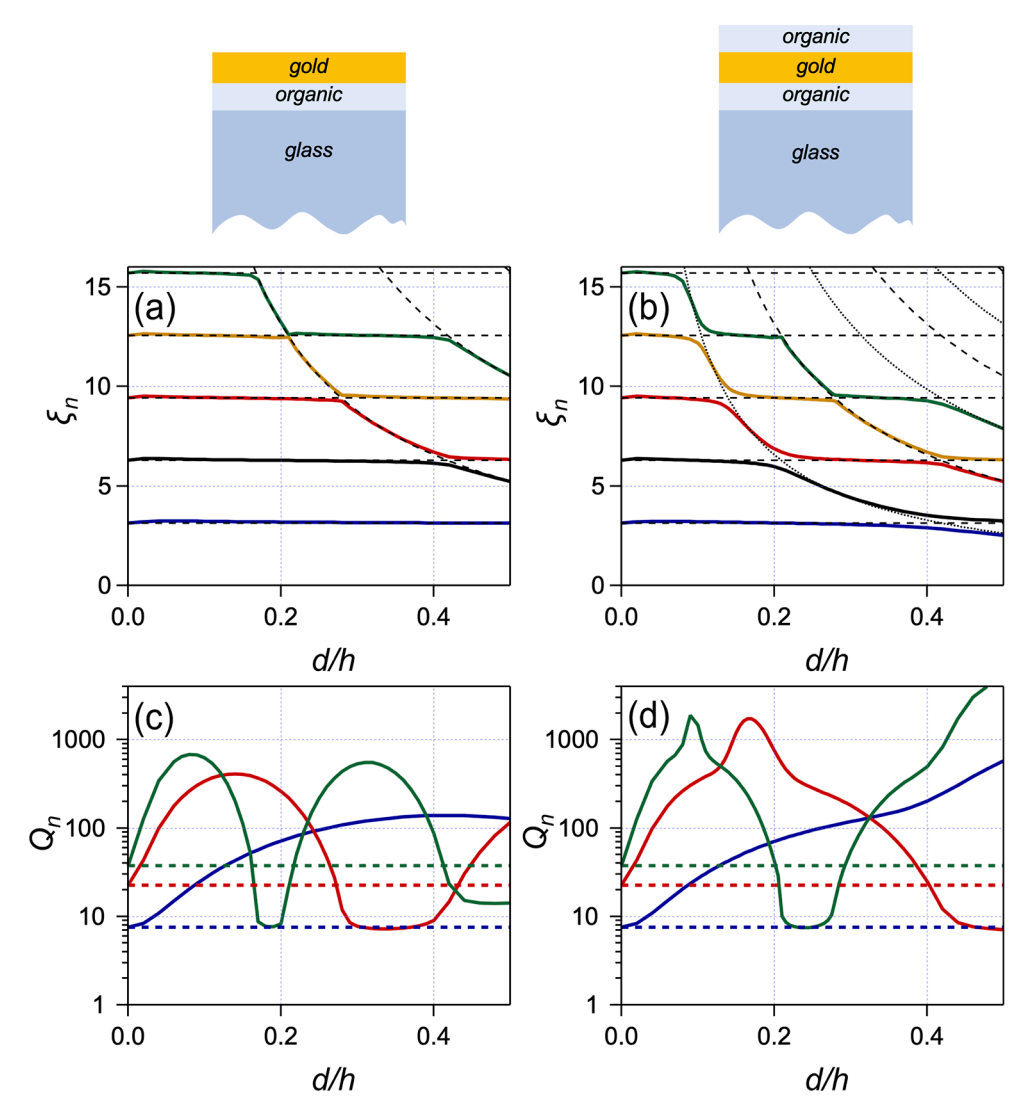


Figure 3. Eigenvalues for a nanoplate on a glass substrate with (a) a single organic spacer layer and (b) with organic layers on the top and bottom of the nanoplate for the n = 1 (blue), n = 2 (black), n = 3 (red), n = 4 (gold), and n = 5 (green) modes. The horizontal dashed lines show the eigenvalues for a free nanoplate, and the curved lines that follow 1/d are the modes for an organic layer with homogeneous (dashed) or mixed boundary conditions (dotted, panel (b) only). The corresponding quality factors are presented in panels (c) and (d) for the n = 1, n = 3, and n = 5 modes (same color scheme as panels (a) and (b)). The horizontal dashed lines in (c) and (d) are the Q_n values for a nanoplate on glass with no spacer layer.

surface without a spacer layer. At small values of d/h the experimental data and the calculations are in good agreement, and both are close to the values expected for a nanoplate in direct contact with the substrate. At larger values of d/h the calculations are in good agreement with the experimental data for the fundamental mode, in both the form of the plot (Q_n) increases with (f_3/f_1) – 3 before reaching a plateau) and the magnitude. The agreement is not as good for the n = 3overtone. However, good agreement between the experimental and calculated quality factors can be achieved for the n=3mode by adding internal damping: that is, by calculating a total quality factor by $1/Q_{tot} = 1/Q_{sub} + 1/Q_{int}$, where Q_{sub} is the damping due to radiation of sound waves into the substrate (which is obtained from eq 2) and Q_{int} is the internal damping contribution.²⁰ The dashed lines in Figure 4 show Q_{tot} for the fundamental and n = 3 overtone for a value of $Q_{int} = 150$. Using this value for Q_{int} brings the experiments and calculations into good agreement for the n = 3 mode; however, the agreement between the experiments and calculations is now slightly worse for the fundamental mode. This may indicate a frequency dependence for the internal damping. Note that the value of internal damping used here is consistent with our previous measurement for the "essentially free" Au nanoplate in ref 13, as well as previous measurements for other Au nanoplate samples.²⁹

The anharmonicity data also allow us to estimate the thickness of the organic layers in these experiments. Figure S3 of the Supporting Information shows a plot of $(f_3/f_1)-3$ versus f_1 . The largest anharmonicities (the most negative values of $(f_3/f_1)-3$) occur at $f_1\approx 20$ GHz, which correspond to nanoplates with thicknesses of approximately 80 nm. Large anharmonicities occur at the avoided crossings between the nanoplate modes and modes of the organic layer. For our system this happens when $\xi_3=3\pi=\frac{1}{2}\pi c_2h/(c_1d)$, which corresponds to $d/h=c_2/(6c_1)\approx 0.14$. This implies a 10 to 11 nm thick organic layer, which is not unreasonable (we presume that the nanoplates in these experiments will be coated with multiple layers of surfactant). Note that we expect

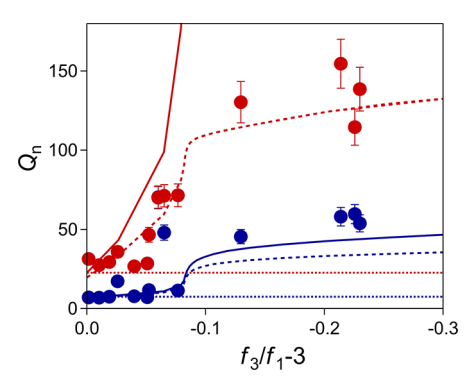


Figure 4. Experimental (points) and calculated quality factors for the fundamental (blue) and n=3 overtone (red) as a function of the relative anharmonicity $(f_3/f_1) - 3$. The horizontal dotted lines show the quality factors for a nanoplate with no substrate, the solid lines are the results calculated using the two layer model (eq 2), and the dashed lines are the calculations with internal damping included ($Q_{int} = 150$).

some heterogeneity in the thickness of the organic layers. This will change the points where the avoided crossings occur, which will affect both the anharmonicity and the quality factors. Plotting the quality factors versus $(f_3/f_1) - 3$ removes this effect to some extent and provides a convenient way to compare theory and experiment.

In conclusion, the fundamental and n = 3 overtones of the thickness vibration of Au nanoplates on a surface have been examined using transient absorption microscopy. The results show that the nanoplate vibrations are in general anharmonic: the frequencies of the overtone modes are not integer multiples of the fundamental frequency as expected for a free nanoplate²³ or a nanoplate directly in contact with a solid substrate. 16,20 A continuum mechanics model consisting of a gold nanoplate on a glass substrate with organic layers on top of the nanoplate and/or between the nanoplate and the substrate was developed to explain these results. Within this model, the anharmonicity arises from coupling between the vibrational modes of the nanoplate and the modes of the organic layers. This creates avoided crossings that reduce the frequencies of the overtone modes relative to the fundamental.²³ This coupling also affects the vibrational quality factors.²⁰ The experiments show that the quality factors of the overtone modes are larger than that of the fundamental modes, which can only be explained by coupling to the top organic layer in the two layer model. Plotting the quality factors versus the scaled frequency (f_3/f_1) – 3, which is a measure of the anharmonicity, provides a way of comparing the experiments and calculations. Good agreement between experiment and theory can be obtained by including a modest amount of internal damping, Q_{int} = 150, which is consistent with previous measurements. 13

These results show that engineering organic layers between the nanoplate and substrate and on top of the nanoplate is a potential way to control vibrational quality factors. Higher quality factors occur when the nanoplate vibrations are coupled to the vibrational modes of the top organic layer. For the n=3 overtone this occurs when the thickness of the organic layer is around 14% of the nanoplate thickness (see Figure 3). The ability to create systems with high quality factors is important for applications such as mass sensing 3,4 and for investigating physical phenomena like vibrational coupling between nanostructures. ¹⁰ It may also be possible to

study how internal damping depends on vibrational frequency using these measurements.³⁰ However, a problem with the current system is the lack of control and/or knowledge of the thickness of the organic layers. The sample in these experiments was created by simply drop casting nanoplates onto a glass surface. The organic layer thus comes from the surfactant that coats the nanoplates in solution, which is not controlled. Current work is focused on creating samples with well-defined organic layers to provide a quantitative test of the theory.

ASSOCIATED CONTENT

Supporting Information

The Supporting Information is available free of charge at https://pubs.acs.org/doi/10.1021/acs.nanolett.3c03660.

Details of the ASOPS experiments, including calculation of the Nyquist interval; data analysis and error estimates for the frequencies and quality factors; description of the continuum mechanics models used, and derivations of eqs 1 and 2 (PDF)

AUTHOR INFORMATION

Corresponding Author

Gregory V. Hartland – Department of Chemistry and Biochemistry, University of Notre Dame, Notre Dame, Indiana 46556, United States; oorcid.org/0000-0002-8650-6891; Email: ghartlan@nd.edu

Author

Cameron Wright — Department of Chemistry and Biochemistry, University of Notre Dame, Notre Dame, Indiana 46556, United States; orcid.org/0000-0002-0122-8168

Complete contact information is available at: https://pubs.acs.org/10.1021/acs.nanolett.3c03660

Author Contributions

CW performed the experiments and analyzed the data; GH developed the continuum mechanics expressions for the vibrational eigenvalues. Both authors contributed to writing the manuscript.

Notes

The authors declare no competing financial interest.

ACKNOWLEDGMENTS

The authors acknowledge the support of NSF through Award CHE-2002300.

REFERENCES

- (1) Crut, A.; Maioli, P.; Del Fatti, N.; Vallee, F. Acoustic vibrations of metal nano-objects: Time-domain investigations. *Phys. Rep.* **2015**, 549, 1–43.
- (2) Chien, M. H.; Brameshuber, M.; Rossboth, B. K.; Schutz, G. J.; Schmid, S. Single-molecule optical absorption imaging by nanomechanical photothermal sensing. *Proc. Natl. Acad. Sci. U.S.A.* **2018**, 115, 11150–11155
- (3) Dominguez-Medina, S.; Fostner, S.; Defoort, M.; Sansa, M.; Stark, A. K.; Halim, M. A.; Vernhes, E.; Gely, M.; Jourdan, G.; Alava, T.; Boulanger, P.; Masselon, C.; Hentz, S. Neutral mass spectrometry of virus capsids above 100 megadaltons with nanomechanical resonators. *Science* 2018, 362, 918–922.

- (4) Sbarra, S.; Waquier, L.; Suffit, S.; Lemaître, A.; Favero, I. Multimode Optomechanical Weighting of a Single Nanoparticle. *Nano Lett.* **2022**, 22, 710–715.
- (5) Fogliano, F.; Besga, B.; Reigue, A.; Mercier de Lépinay, L.; Heringlake, P.; Gouriou, C.; Eyraud, E.; Wernsdorfer, W.; Pigeau, B.; Arcizet, O. Ultrasensitive nano-optomechanical force sensor operated at dilution temperatures. *Nat. Commun.* **2021**, *12*, 4124.
- (6) Yu, K.; Yang, Y.; Wang, J. Z.; Hartland, G. V.; Wang, G. P. Nanoparticle-Fluid Interactions at Ultrahigh Acoustic Vibration Frequencies Studied by Femtosecond Time-Resolved Microscopy. *ACS Nano* **2021**, *15*, 1833–1840.
- (7) Unterreithmeier, Q. P.; Faust, T.; Kotthaus, J. P. Damping of Nanomechanical Resonators. *Phys. Rev. Lett.* **2010**, *105*, No. 027205.
- (8) Schmid, S.; Jensen, K. D.; Nielsen, K. H.; Boisen, A. Damping mechanisms in high-Q micro and nanomechanical string resonators. *Phys. Rev. B* **2011**, *84*, No. 165307.
- (9) Seitner, M. J.; Gajo, K.; Weig, E. M. Damping of metallized bilayer nanomechanical resonators at room temperature. *Appl. Phys. Lett.* **2014**, *105*, No. 213101.
- (10) Wang, J.; Yu, K.; Yang, Y.; Hartland, G. V.; Sader, J. E.; Wang, G. P. Strong vibrational coupling in room temperature plasmonic resonators. *Nat. Commun.* **2019**, *10*, 1527.
- (11) Medeghini, F.; Crut, A.; Gandolfi, M.; Rossella, F.; Maioli, P.; Vallee, F.; Banfi, F.; Del Fatti, N. Controlling the Quality Factor of a Single Acoustic Nanoresonator by Tuning its Morphology. *Nano Lett.* **2018**, *18*, 5159–5166.
- (12) Hettich, M.; Jacob, K.; Ristow, O.; Schubert, M.; Bruchhausen, A.; Gusev, V.; Dekorsy, T. Viscoelastic properties and efficient acoustic damping in confined polymer nano-layers at GHz frequencies. *Sci. Rep.* **2016**, *6*, No. 33471.
- (13) Wright, C.; Hartland, G. V. Mode specific dynamics for the acoustic vibrations of a gold nanoplate. *Photoacoustics* **2023**, *30*, No. 100476.
- (14) Noll, F.; Krauß, N.; Gusev, V.; Dekorsy, T.; Hettich, M. Surface plasmon-based detection for picosecond ultrasonics in planar gold-dielectric layer geometries. *Photoacoustics* **2023**, *30*, No. 100464.
- (15) Tchebotareva, A. L.; Ruijgrok, P. V.; Zijlstra, P.; Orrit, M. Probing the acoustic vibrations of single metal nanoparticles by ultrashort laser pulses. *Laser & Photonics Reviews* **2010**, *4*, 581–597.
- (16) Fedou, J.; Viarbitskaya, S.; Marty, R.; Sharma, J.; Paillard, V.; Dujardin, E.; Arbouet, A. From patterned optical near-fields to high symmetry acoustic vibrations in gold crystalline platelets. *Phys. Chem. Chem. Phys.* **2013**, *15*, 4205–4213.
- (17) Su, M. N.; Ostovar, B.; Gross, N.; Sader, J. E.; Chang, W. S.; Link, S. Acoustic Vibrations and Energy Dissipation Mechanisms for Lithographically Fabricated Plasmonic Nanostructures Revealed by Single-Particle Transient Extinction Spectroscopy. *J. Phys. Chem. C* **2021**, *125*, 1621–1636.
- (18) Beane, G.; Devkota, T.; Brown, B. S.; Hartland, G. V. Ultrafast measurements of the dynamics of single nanostructures: a review. *Rep. Prog. Phys.* **2019**, 82, No. 016401.
- (19) Gross, N.; Madadi, M.; Ostovar, B.; Dongare, P. D.; McCarthy, L. A.; Chiang, W.-Y.; Chang, W.-S.; Halas, N. J.; Landes, C. F.; Sader, J. E.; Link, S. Strong Substrate Binding Modulates the Acoustic Quality Factors in Gold Nanodisks. *J. Phys. Chem. C* **2023**, *127*, 5054–5066.
- (20) Yu, K.; Jiang, Y. Q.; Wright, C.; Hartland, G. V. Energy Dissipation for Nanometer Sized Acoustic Oscillators. *J. Phys. Chem.* C 2022, 126, 3811–3819.
- (21) Bartels, A.; Cerna, R.; Kistner, C.; Thoma, A.; Hudert, F.; Janke, C.; Dekorsy, T. Ultrafast time-domain spectroscopy based on high-speed asynchronous optical sampling. *Rev. Sci. Instrum.* **2007**, *78*, No. 035107.
- (22) Asahara, A.; Arai, Y.; Saito, T.; Ishi-Hayase, J.; Akahane, K.; Minoshima, K. Dual-comb-based asynchronous pump-probe measurement with an ultrawide temporal dynamic range for characterization of photo-excited InAs quantum dots. *Appl. Phys. Exp.* **2020**, *13*, No. 062003.

- (23) Lerme, J.; Margueritat, J.; Crut, A. Vibrations of Dimers of Mechanically Coupled Nanostructures: Analytical and Numerical Modeling. *J. Phys. Chem. C* **2021**, *125*, 8339–8348.
- (24) Crut, A. Substrate-supported nano-objects with high vibrational quality factors. *J. Appl. Phys.* **2022**, *131*, No. 244301.
- (25) Yu, K.; Devkota, T.; Beane, G.; Wang, G. P.; Hartland, G. V. Brillouin Oscillations from Single Au Nanoplate Opto-Acoustic Transducers. *ACS Nano* **2017**, *11*, 8064–8071.
- (26) Gusev, V. E.; Ruello, P. Advances in applications of time-domain Brillouin scattering for nanoscale imaging. *Appl. Phys. Rev.* **2018**, *5*, No. 031101.
- (27) Mongin, D.; Juvé, V.; Maioli, P.; Crut, A.; Del Fatti, N.; Vallée, F.; Sánchez-Iglesias, A.; Pastoriza-Santos, I.; Liz-Marzán, L. M. Acoustic Vibrations of Metal-Dielectric Core—Shell Nanoparticles. *Nano Lett.* **2011**, *11*, 3016–3021.
- (28) Fernandes, B. D.; Vilar-Vidal, N.; Baida, H.; Massé, P.; Oberlé, J.; Ravaine, S.; Treguer-Delapierre, M.; Saviot, L.; Langot, P.; Burgin, J. Acoustic Vibrations of Core—Shell Nanospheres: Probing the Mechanical Contact at the Metal—Dielectric Interface. *J. Phys. Chem. C* 2018, 122, 9127—9133.
- (29) Wang, J.; Yang, Y.; Wang, N.; Yu, K.; Hartland, G. V.; Wang, G. P. Long Lifetime and Coupling of Acoustic Vibrations of Gold Nanoplates on Unsupported Thin Films. J. Phys. Chem. A 2019, 123, 10339—10346.
- (30) Lifshitz, R.; Roukes, M. L. Thermoelastic damping in microand nanomechanical systems. *Phys. Rev. B* **2000**, *61*, 5600–5609.